Multi-anticipative driving strategies in microscopic traffic models

Martin Treiber,* Arne Kesting,† and Dirk Helbing‡
Institute for Economics and Traffic, Dresden University of Technology,
Andreas-Schubert-Str. 23, 01062 Dresden, Germany
(Dated: March 15, 2004)

We formulate several key aspects of human driving dynamics based on a wide class of time-continuous microscopic traffic models. In the underlying models such as the intelligent-driver model (IDM) or the optimal velocity model, the acceleration response is instantaneous and depends only on the own vehicle and its predecessor therefore resembling (semi-)automated driving rather than human driving. We propose generalizations to include the essential differences of human drivers with respect to these models, specifically (i) finite reaction times, (ii) errors in estimating the input variables, (iii) looking several vehicles ahead (spatial anticipation), (iv) estimating the future traffic situation (temporal anticipation), and (v) long-term adaptation to the global traffic situation (memory effect). By means of simulations with the IDM as base model we show that the destabilizing effects of reaction times and estimation errors can be offset to a large extent by the spatial and temporal anticipations resulting in the same stability and qualitative macroscopic dynamics as that of the IDM. Accident-free smooth driving is possible even for reaction times exceeding the time headway. An analysis of virtual detector data of simulated congested traffic shows that the combined effect of the anticipations lead to smaller velocity gradients and, in case of oscillating congested traffic, to longer periods of the oscillations, in agreement with real traffic. Furthermore, the model allows to simulate the transition free traffic → synchronized traffic → traffic jams and to reconcile the three-phase theory proposed by Kerner with the phase diagram proposed by Helbing.

PACS numbers: 05.60.-k, 05.70.Fh, 47.55.-t, 89.40

I. INTRODUCTION

The nature of human driving behaviour and the differences to automated driving that is implemented implicitely by most micromodels is a controversial topic in traffic science [1–3]. Finite reaction times, finite estimation capabilities and limited attention spans impair the human driving performance and stability with respect to automated driving, sometimes called adaptive cruise control (ACC). However, unlike machines, human drivers routinely scan the traffic situation several vehicles ahead ("multi-anticipation" [4–6]) and anticipate future traffic situations [7] leading, in turn, to an increased stability. The question arises how these antagonistic effects affect the overall driving behaviour and performance, and whether, in typical situations, the stabilizing or the destabilizing effects dominate, or if they effectively cancel each other. The answers to these questions are crucial in determining the influence of the growing number of vehicles equipped with automated acceleration controls on the overall traffic flow. Up to now, there is not even clarity about the sign of the effect. Some investigations predict a positive effect [8] while others are more pessimistic [9] **CHECK Literatur, v.a. TRB**

Individual aspects of human driving behaviour have been investigated in the past. For example, it is well known that traffic instabilities increase with the reaction times of the drivers. Finite reaction times in time-continuous micromodels have been modelled as early as 1961 by Newell [10] and, recently, the optimal-velocity model (OVM) [11] has been extended to include finite reaction times [12]. However, the Newell model has no dynamic velocity, and the OVM with delay turned out to be accident-free only for irrealistically small reaction times [13]. To overcome this deficiency, Davis [7, 14] introduced (among other modifications) an anticipation of the expected future gap to the front vehicle allowing accident-free driving at reaction times of 1 s. However, reaction times were not fully implemented in [7, 14] since the own velocity, which is one of the stimuli on the right-hand side of the acceleration equation, has been taken at the actual rather than at the delayed time. Furthermore, in some traffic situations such as stop-and-go traffic, after active or passive lane changes, or when simply accelerating on an empty road, the OVM leads to unrealistically high accelerations (of the order of $v_0/\tau = 30$ m/s^{2}for typical values $v_0 = 30$ m/s for the desired velocity and $\tau = 1$ s for the velocity relaxation time). To our knowledge, there exists no car-following model exhibiting string stability for reaction times (with respect to all stimuli) exceeding half of the time headway of the platoon vehicles. Human drivers, however, accomplish this easily. In dense (not congested) traffic, the most probable time headways are 0.9-1s [15] which is of the same order as typical reaction times [**?**]. **SUCHE Referenz, in Transp. Res. F oder in Referenzen der Davis-Paper**

Possibly, human drivers achieve this stability by con-

*Electronic address: martin@mtreiber.de; URL: http://www.mtreiber.de
†Electronic address: mail@akesting.de
‡Electronic address: helbing@trafficforum.org; URL: http://www.helbing.org

sidering not only the vehicle immediately in front but also to next-nearest neighbours and further vehicles ahead which we will denote by "spatial anticipation" or "multi-anticipation" [4]. Spatial anticipation has been applied to the OVM [4] and to the Gipps model [5] As expected, the resulting "multi-anticipativ" models show more stability compared to the original model. However, the stability of the aforementioned models is yet less than that of human drivers. Furthermore, some unrealistic behaviour emerge such as too high backwards propagation velocities ($v_g = -30$ km/h) of perturbations in congested traffic [4].

Besides reacting to the immediate traffic environment, human drivers adapt their driving style on a longer time scale to the traffic situation [16] such that the actual driving style depends on the traffic conditions of the last few minutes (memory effect [17]). For example, most drivers increase the time headways to the leading vehicle after some time in congested traffic [16, 18] which is sometimes termed "resignation effect" [19, 20]. **doppelter Eintrag "Katsu03" in der Datenbank. Ein Beitrag bezieht sich auf cond-mat; diesen bitte in "Katsu03-condmat" umbenennen**

Imperfect estimation capabilities often serve as motivation or justification to introduce stochastic terms into micromodels such as the Gipps model [21] (see also [1, 22]). Most cellular automata require fluctuating terms as well. In nearly all the cases, fluctuations are assumed to be δ-correlated in time and acting directly on the accelerations. An important feature of human estimate errors, however, is a certain persistency. If one underestimates, say, the distance at time t, the propability of underestimating it at the next time step (which typically is less than 1 s in the future) is very high as well. We are not aware of any work where this obvious temporal correlation has been taken into account.

In this paper, we propose a human driver model (HDM) that incorporates all of the above aspects. The model allows accident-free driving with realistic accelerations in nearly all traffic situations (including driving on empty roads and approaching standing obstacles) for reaction times of the order of and even slightly exceeding the time headway. On a macroscopic level, the model can produce all the congested traffic phases of the phase diagram of Helbing and Treiber [23] but also the transition "free traffic → synchronized traffic → jams" proposed by Kerner [24] thus possibly allowing to reconcile the two opposing views [25].

In Sec. II, we formulate the HDM in terms of extensions for a class of micromodels where the acceleration is a continuous function of the velocity, the gap, and the velocity of the preceding car. We use the intelligent-driver model (IDM) [26] as underlying model since it has already a built-in anticipative and smooth braking strategy and scored best in a first independent attempt to benchmark micromodels on real traffic data [27]. Other popular models which may serve as underlying model are the OVM [11], the Gipps model [28] or the boundedly rational driver model [29, 30].

In Sec. III we simulate the stability of vehicle platoons as a function of reaction time T' and number of anticipated vehicles n_a and found string stability for arbitrarily long platoons for reaction times of up to 1.5 s. We show that both spatial and temporal anticipations play a crucial role. Furthermore, we simulate the macroscopic effects for an open system containing a flow-conserving bottleneck [26, 31, 32]. We found that multi-vehicle anticipation ($n_a > 1$) can offset the destabilizing effects of reaction times and estimate errors and plot a phase diagram for the corresponding parameter space. When increasing simultaneously T' and n_a such that the stability is constant, we found that the wavelength of stop-and go waves increased and the fronts between free and congested traffic became smoother, in accordance to observations.

In the concluding Section IV we suggest applications and further investigations and discuss some aspects of human driving that are not included in the HDM.

II. MODELLING HUMAN DRIVING BEHAVIOUR

In this paper, we use the intelligent-driver model (IDM) [26] as underlying micromodel. We will formulate the various aspects of human driving in a model-independent way, so other longitudinal time-continuous micromodels such as the optimal-velocity model [11] or the Gipps model [21] can be applied as well. Furthermore, we restrict to single-lane traffic here. Lane-change related aspects of human driving will be investigated in a forthcoming work.

In the following, we recapitulate shortly the most important aspects of the IDM. In this model, the acceleration of each vehicle α is assumed to be a continuous function of the velocity v_α, the netto distance gap s_α, and the velocity difference (approaching rate) Δv_α to the leading vehicle:

$$\dot{v}_\alpha = a\left[1 - \left(\frac{v_\alpha}{v_0}\right)^4 - \left(\frac{s^*(v_\alpha, \Delta v_\alpha)}{s_\alpha}\right)^2\right]. \qquad (1)$$

This expression is an interpolation of the tendency to accelerate with $a_f(v) := a[1 - (v/v_0)^4]$ on a free road and the tendency to brake with deceleration $-b_{\rm int}(s, v, \Delta v) := -a(s^*/s)^2$, when vehicle α comes too close to the vehicle in front. The deceleration term depends on the ratio between the effective "desired minimum gap" s^* and the actual gap s_α, where the desired gap

$$s^*(v, \Delta v) = s_0 + vT + \frac{v\Delta v}{2\sqrt{ab}} \qquad (2)$$

is dynamically varying with the velocity. The minimum distance s_0 in jams is significant for low velocities only. The main contribution in stationary traffic is the term

vT which corresponds to following the preceding vehicle with a constant "safety" netto time gap T. The last term is only active in non-stationary traffic and implements an accident-free "intelligent" driving behaviour including a braking strategy that, in nearly all situations, limits braking decelerations to the "comfortable deceleration" b.

As most other microscopic traffic models, the IDM describes an automated driving control system rather than human drivers since it presumes (i) instantaneous reaction, (ii) reaction only to the immediate predecessor, (iii) infinitely exact estimating capabilities of the input quantities s, v, and Δv, and (iv) no long-term adaptation to the global traffic situation. By virtue of the "intelligent" braking term in (2), the IDM does contain some temporal anticipation. In the following, we implement the mentioned aspects of human driving.

A. Finite reaction time

We consider underlying microscopic models of the general form

$$\frac{d}{dt}v_\alpha = a^{\rm mic}\left(s_\alpha, v_\alpha, \Delta v_\alpha\right), \tag{3}$$

where the own velocity and distance and velocity difference to the leading vehicle serve as stimuli determining the acceleration [33]. A reaction time T' is implemented simply by taking the right-hand side of Eq. (3) at time $t - T'$. It is essential to distinguish the reaction time T' from the time-headway (parameter T in case of the IDM), and from the update time step dt of the explicit numerical integration. If T' is not a multiple of the update time step, we used a linear interpolation according to

$$x(t - T') = \beta x_{t-n-1} + (1 - \beta)x_{t-n}, \tag{4}$$

where x denotes any quantity s_α, v_α, or Δv_α of the right-hand side of (3), x_{t-n} denotes this quantity taken $n = \text{floor}\,(T'/dt)$ time steps before the actual step, and the weighting factor is given by $\beta = T'/dt - n$. Notice that *all* input stimuli, including the velocity, are taken at the delayed time.

B. Imperfect estimation capabilities

We will model estimating errors for the netto distance s and the velocity difference Δv to the preceding vehicle. Since the velocity itself can be obtained by looking at the speedometer, we neglect its estimating error. From empirical investigations (for an overview see [1], p. 190) it is known that the uncertainty of the estimation of Δv is proportional to the distance, i.e., one can estimate the inverse of the time-to collision (TTC) $|\Delta v|/s$ with a constant uncertainty [34]. For the distance itself, we base the estimation error on a relative scale, i.e., assume a constant variation coefficient V_s of the errors. Furthermore, we want to take into consideration that, obviously, estimation errors have a certain correlation time which can be modelled by a Wiener process [35]. This leads to following nonlinear stochastic processes for the distance and the velocity difference,

$$s^{\rm est}(t) = s(t)\ \exp(V_s w_s(t)), \tag{5}$$

and

$$(\Delta v)^{\rm est}(t) = \Delta v + s(t)\ r_{\rm c} w_{\Delta v}(t), \tag{6}$$

where V_s is the variation coefficient of the distance estimate, and $r_{\rm c}$ the inverse TTC as measure of the error in Δv. The stochastic variables $w_s(t)$ and $w_{\Delta v}(t)$ obey independent Wiener processes $w(t)$ of variance 1 with correlation times $\tau = \tau_s$ and $\tau_{\Delta v}$, respectively, defined by [35]

$$\frac{dw}{dt} = \frac{-w}{\tau} + \xi(t), \tag{7}$$

with

$$\langle \xi \rangle = 0, \quad \langle \xi(t)\xi(t') \rangle = \frac{2}{\tau}\delta(t - t'). \tag{8}$$

In the explicit numerical update from time step t to step $t + 1$, we implemented the Wiener processes by the approximations

$$w_{t+1} = e^{-dt/\tau} w_t + \sqrt{\frac{2dt}{\tau}}\eta_t \tag{9}$$

where the $\{\eta_t\}$ are independent realizations of a Gaussian distributed quantity of zero mean and unit variance. We checked numerically that update scheme (9) satisfies the fluctuation-dissipation theorem $\langle w_t^2 \rangle = 1$ for any update time step satisfying $dt \ll \tau$.

C. Temporal anticipation

Besides the braking term of the IDM implementing an anticipative braking strategy we assume that drivers are aware of their finite reaction time and anticipate the traffic situation accordingly. Besides anticipating the future distance [14] we will anticipate the future velocity using a constant-acceleration heuristics. The combined effects of a finite reaction time, estimation errors and temporal anticipation leads to following input variables for the underlying micromodel (3),

$$\frac{dv}{dt} = a^{\rm mic}(s'_\alpha, v'_\alpha, \Delta v'_\alpha), \tag{10}$$

with

$$s'_\alpha(t) = \left[s_\alpha^{\rm est} - T'\Delta v_\alpha^{\rm est}\right]_{t-T'}, \tag{11}$$

$$v'_\alpha(t) = \left[v_\alpha^{\rm est} + T' a_\alpha\right]_{t-T'}, \tag{12}$$

and

$$\Delta v'_\alpha(t) = \Delta v_\alpha^{\rm est}(t - T'). \tag{13}$$

D. Spatial anticipation several vehicles ahead

We assume that the acceleration of the underlying microscopic model can be split into a single-vehicle acceleration valid on a nearly empty road which depends only on the considered vehicle α, and a two-vehicle braking deceleration taking into account the vehicle-vehicle interaction with the preceding vehicle,

$$a^{\rm mic}(s_\alpha, v_\alpha, \Delta v_\alpha) := a_\alpha^{\rm free} + a^{\rm int}(s_\alpha, v_\alpha, \Delta v_\alpha). \qquad (14)$$

Notice that this split of the acceleration has already been used to formulate a lane-changing model for a wide class of micromodels [36]. **Bitte Referenz "MOBIL" in die Dtaenbank eintragen: Author: Martin Treiber und Dirk Helbing Title: Realistische Mikrosimulation von Straenverkehr mit einem einfachen Modell Proceedingsband: 16. Symposium "Simulationstechnik" ASIM 2002 Rostock, 10.09 - 13.09.2002 Tagungsband, Hrsg. Djamshid Tavangarian und Rolf Grützner S. 514–520**

We model reaction to several vehicles ahead just by summing up the corresponding vehicle-vehicle pair interactions $a_{\alpha\beta}^{\rm int}$ from vehicle β to vehicle α,

$$a_{\alpha\beta}^{\rm int} = a^{\rm int}\left(\sum_{j=\beta-1}^{\alpha} s_j, v_\alpha, v_\alpha - v_\beta\right), \qquad (15)$$

for the $n_{\rm a}$ nearest preceding vehicles β. Thus, the combination of all effects discussed up to now can be modelled by

$$\frac{d}{dt}v_\alpha(t) = a_\alpha^{\rm free} + \sum_{\beta=\alpha-n_{\rm a}}^{\alpha-1} a_{\alpha\beta}^{\rm int}, \qquad (16)$$

where all distances, velocities and velocity differences on the right-hand sides are given by (11) - (13).

Renormalisation for the IDM

For the IDM, there exists a closed-form solution of the multi-anticipative equilibrium distance as a function of the velocity,

$$s_e(v) = \gamma s^*(v,0)\left[1-\left(\frac{v}{v_0}\right)^\delta\right]^{-\frac{1}{2}}, \qquad (17)$$

which is γ times the equilibrium distance of the original IDM [26] where

$$\gamma = \sqrt{\sum_{i=1}^{n_{\rm a}} \frac{1}{i^2}}. \qquad (18)$$

The equilibrium distance $s_e(v)$ can be transformed to that of the original IDM by renormalizing the relevant IDM parameters appearing in $s^*(v,0)$,

$$s_0^{\rm ren} = \frac{s_0}{\gamma}, \quad T^{\rm ren} = \frac{T}{\gamma} \qquad (19)$$

Intuitively this means that a smaller part of the next-neighbour (NN) interaction is redistributed to create the non-NN interactions. The above renormalisation will be applied to all simulations of this paper.

Notice that in the limiting case of anticipation to arbitrary many vehicles we obtain $\lim_{n_{\rm a}\to\infty}\gamma(n_{\rm a}) = \pi/\sqrt{6} = 1.283$. Thius means that the combined effects of all non-NN interactions would lead to an increase of the equilibrium distance by just about 28%.

Parameter	Value
Desired velocity $v_0 = v_{0,\max}$	128 km/h
Save time headway $T = T_{\min}$	1.1 s
Maximum acceleration a	1 m/s^2
Desired deceleration b	1.5 m/s^2
Acceleration exponent δ	4
Jam distance s_0	2 m

TABLE I: Model parameters of the IDM as used in this paper. The vehicle length is 5 m. The the string stability szenario, v_0 and T are adopted to the parameters used in [13].

E. Adaptation of the driving style to the traffic environment

It is observed that most drivers, after being stuck for some time in congested traffic, increase their preferred temporal headway [16, 37]. Furthermore, when larger gaps appear or when reaching the downstream front of the congested zone, human drivers accelerate less and possibly decrease their desired velocity with respect to a free-traffic situation.

We model this *memory effect* [17] by assuming that, when encountering congested traffic characterized by a low "level-of service" $\lambda = v_\alpha/v_0$ drivers gradually decrease their acceleration parameter a to a value $a(\lambda) = a[1+(1-\lambda)(\beta_a-1)]$ and increase the time headway T (in case of the IDM, $T^{\rm ren}$) to $T(\lambda) = T[1+(1-\lambda)(\beta_T-1)]$. The adaptations take place on a time scale τ of the order of a few minutes. Further details are given in [17].

III. SIMULATIONS AND RESULTS

Unless stated otherwise, we will use the values of the IDM parameters given in Table I and that of the HDM given in Table II. Notice that all human-driver extensions are switched off (i.e., the IDM is recovered) for the HDM values $T' = 0$, $V_s = 0$, $r_c = 0$, $n_a = 1$, and $\beta_a = \beta_T = 1$.

Parameter	value
Reaction time T'	0 s - 1.5 s
Number of anticipated vehicles n_a	1 - 8
Relative distance error V_s	5%
Inverse TTC error r_c	0.01/s
error correlation times τ_s, $\tau_{\Delta v}$	20 s
Traffic adaptation factor β_a	0.5
Traffic adaptation factor β_T	1.3
Traffic adaptation time τ	120 s

TABLE II: CHECK WERTE! Parameters of all human-driver extensions with values used in this paper.

A. String Stability of a platoon

We investigated the stability limit of the HDM with respect to reaction time T' and number n_a of anticipated vehicles by simulating a platoon of 100 vehicles following an externally controlled lead vehicle. As in a similiar study on the OVM [13, 14], the lead vehicle drives at $v_{\rm lead} = 15.34\,{\rm m/s}$ for the first 1000 s before it decelerates with $-0.7\ {\rm m/s}^2$ to 14.0 m/s and drives at this velocity until the simulation ends at 2500 s.

For the platoon vehicles, we set the IDM parameters $v_0 = 32\,{\rm m/s}$ and $T = 1.5\,{\rm s}$ to obtain the same desired velocity and initial equilibrium distance ($s_{\rm e} = 25.7\,{\rm m}$) as in the studies [13, 14]. The other IDM parameters are that of Table I. If n_a is larger than the number of preceding vehicles (which can happen for the first vehicles of the platoon) then n_a is reduced accordingly. Neither fluctuations nor memory effects have been activated in this scenario. As initial conditions, we assumed the platoon to be at equilibrium.

We distinguish three stability regimes. (i) String stability, i.e., all perturbations introduced by the deceleration of the lead vehicles are damped away, (ii) an oscillatory regime, where perturbations increase but do not lead to crashes, (iii) instability with crashes. Oscillating behaviour was detected if the maximum deceleration of all vehicle in all timesteps exceeded $2\ {\rm m/s}^2$. Figure 1 shows the three phases depending on the reaction time T' and on the platoon size for spatial anticipations of $n_a = 1$ and 5 vehicles, respectively.

For $n_a = 1$ (corresponding to conventional car-following models without spatial anticipation), a platoon of 100 vehicles is stable for reaction times of up to $T'_{\rm c1} = 0.8\,{\rm s}$. Test runs with larger platoon sizes (up to 1000 vehicles did not result in different thresholds suggesting that stability for a platoon size of 100 essentially means stability for arbitrarily large platoon sizes.

Increasing the spatial anticipation to $n_a = 5$ vehicles shifted the threshold of the delay time T' for string stability of a platoon of 100 vehicles to $T'_{\rm c1} = 1.3\,{\rm s}$. Increasing the delay time T' beyond the stability threshold lead to strong oscillations of the platoon. Crashes, however, occurred only when T' is above a second threshold $T'_{\rm c2}$. Remarkably, for $n_a = 5$ or more vehicles, the observed

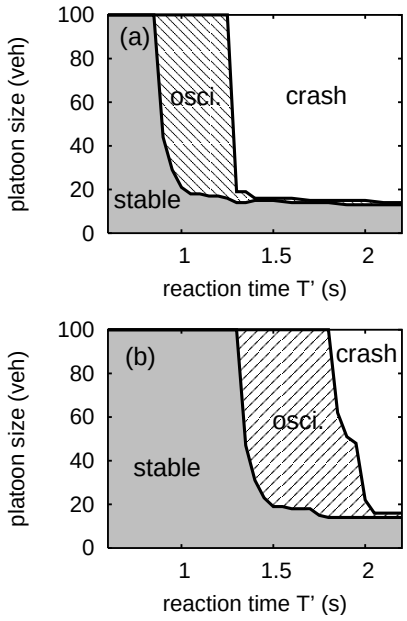

FIG. 1: Stability of a platoon of identical vehicles as a function of the platoon size and the reaction time T' for the situation described in Section III A (a) for spatial anticipation $n_a = 1$, and (b) for $n_a = 5$. In the "stable" phase, all perturbations are damped away. In the oscillatory regime, the perturbations increase but do not lead to crashes.

threshold $T'_{\rm c2} = 1.8\,{\rm s}$ is larger than the equilibrium time headway $s_e/v_{\rm lead} = 1.68$ s. More detailled investigations revealed that the crashes are triggered either directly by late reactions to the deceleration maneuver or indirectly as a consequence of the string instabilites. Further increase of n_a did not change the thresholds significantly.

In the simulations above, the update time step of the numerical (Euler) integration scheme has been $\Delta t = 0.1$ s, i.e., small compared to T'. Since both finite reaction times and update time steps act as a delay, we expect similar dynamical effects for simulations with $T' = 0$ and Δt of the order of the thresholds $T'_{\rm c1}$ or $T'_{\rm c2}$.

We systematically investigated the effects of various combinations of T' and ΔT for a platoon size of 100 vehicles. Figure 2 shows the result in form of a phase diagram spanned by both times. For $T' = 0$ and $n_a = 1 (n_a = 5)$, we observed stable platoon behaviour for $\Delta t \leq 1.5$ s ($\Delta t = 2.5$ s), i.e., clearly larger than the corresponding threshold values $T'_{\rm c1}$ of the reaction times, cf. Fig. 1. This is plausible, since the effective delay introduced by finite update time steps varies between zero at times $t = (n + \epsilon)\Delta t$ with $n \in \mathbb{N}$ and $\epsilon \ll 1$ (immediately after an update time step), and ΔT at time $t = (n + 1 - \epsilon)\Delta t$ (immediately before the next update).

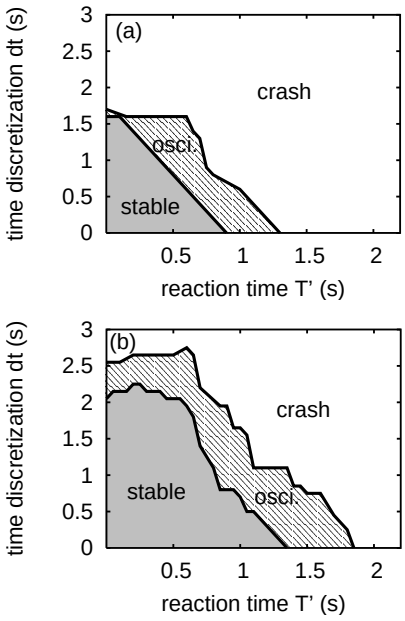

FIG. 2: The three dynamical phases for a platoon size of 100 as a function of reaction time and numerical time discretization (a) for a spatial anticipation of $n_a = 1$ and (b) for $n_a = 5$.

B. Open system with a bottleneck

In this section we examine the compensating influences of driver reaction times T' and spatial anticipation n_a on the stability of traffic and the occuring traffic states in a more complex and realistic situation.

We have simulated a single-lane road section (total length 20 km) with a bottleneck and open boundaries. We assumed identical drivers and vehicles of length $l = 5$ m whose HDM parameters (with the exception of T' and n_a) are given by Table II. The update time step of the numerical integration was $\Delta t = 0.2$ s. Each simulation run covered a time interval of 3 h. We initialized the simulations with very light traffic (traffic density 1 vehicle/km) and set all initial velocities to 100 km/h. Notice that the initial conditions are relevant only for the time interval needed for the vehicles to cross the road section, i.e., for about the first 15 min.

We simulated idealized rush-hour conditions by increasing the inflow at the upstream boundary linearly from 0 veh/h at $t = 0$ to 1800 veh/h at $t = 1$ h. For the next 8 min we linearly increased the inflow to 2400 veh/h and afterwards decreased it for the next 8 min to a flow of 1900 veh/h which is kept constant for the rest of the simulation (cf. inset of Fig. 3). Since, at the bottleneck, the maximum inflow $Q_{\max} = 2400$ veh/h exceeds the static road capacity (maximum of the fundamental diagram), a traffic breakdown is always provoked, even for values of T' and n_a corresponding to stable traffic. Both the initial vehicles and the vehicles of the inflow have been initialized with a "memory" of free traffic, cf. **??**.

We have implemented a flow-conserving bottleneck by locally increasing the IDM parameter T from 1.1 s to 1.65 s according to

$$T = T(x) = \begin{cases} \text{linear increase}, & 18.0\,\text{km} \leqslant x \leqslant 18.5\,\text{km} \\ 1.65\,\text{s}, & 18.5\,\text{km} \leqslant x \leqslant 19.5\,\text{km} \\ \text{linear decrease}, & 19.5\,\text{km} \leqslant x \leqslant 20.0\,\text{km} \\ 1.1\,\text{s}, & \text{otherwise.} \end{cases} \tag{20}$$

This corresponds to lowering the road capacity and is representative for any bottleneck that is not an on- or an off-ramp [38].

1. *Phase diagram*

We performed simulation runs with various combinations of the number of anticipated vehicles, $n_a = 1, \ldots, 8$ and reaction times, $T' = 0, \ldots, 1.6$ s. Figure 3 shows the resulting dynamic traffic regimes in the space spanned by n_a and T'.

The left lower corner corresponds to the special case of the IDMM, i.e., zero reaction time and taking into account only the immediate front vehicle. In this case, the simulation leads to oscillatory congested traffic (OCT), cf. Figures 4(a), 5(a), and 6(a). In the OCT state, congested traffic is linearly unstable and small perturbations grow while travelling backwards [23].

Varying n_a and T' lead to following main results: (i) Traffic stability increases drastically when increasing the spatial anticipation from $n_a = 1$ to values ≤ 5 while the stability remains essentially unchanged when increasing n_a further to values > 5. In particular, for a sufficiently large number of anticipated vehicles, the congestion becomes stable (HCT, homogeneous congested traffic) as shown in Fig. 4(b). Thus, different traffic states can be produced not only by varying the bottleneck strength as in the phase diagram proposed first in [23] but also by varying model parameters that influence the stability. (ii) Increasing the reaction time T' destabilizes traffic and finally leads to crashes. For a given n_a, the critical threshold T'_{c2} for crashes is somewhat lower than in the simulations of Sec. III A which is caused by the more complex scenario and by the higher braking decelerations caused by the traffic breakdown. (iii) The other dynamic congested traffic states of the phase diagram of Ref. [23] are found as well, specifically, triggered stop-and-go waves (TSG), cf. Figures 4(c), 5(b), and 6(b), and a combination of moving localized clusters (MLC) and pinned localized clusters (PLC), cf. Fig. 4(d).

Remarkably, the destabilizing effects of finite reaction times can be offset to a large extent by the spatial and temporal anticipation heuristics of the HDM such that the resulting stability dynamics is similar to the IDM(M) case of zero anticipation and reaction time. This is illustrated by comparing Fig. 4(a) (no reaction time and no anticipation) with Fig. 4(c) (finite reaction time and anticipation). Notice, however, that in the simulation of

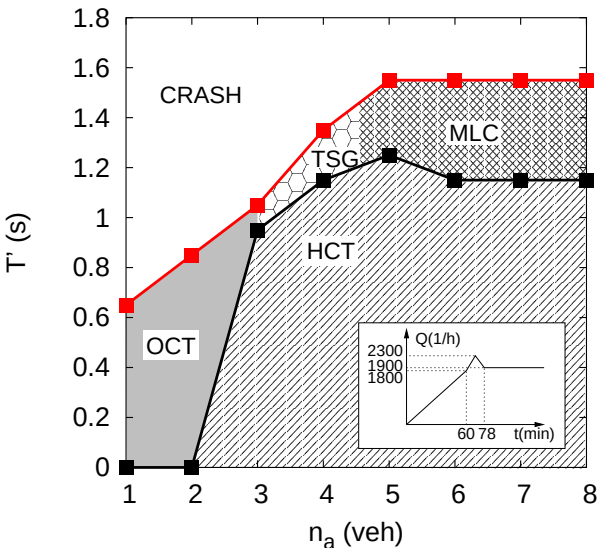

FIG. 3: Phase diagram of congested traffic states in a space spanned by the number of anticipated vehicles and the reaction time. Homogeneous congested traffic (HCT) corresponds to stability also in the congested regime. The other states OCT (oscillatory congested traffic), TSG (triggered stop-and go traffic), and MLC (moving localized traffic) are discussed in the main text.

Fig. 4(c), congested traffic is unstable but convectively stable. Thus, small perturbations induced by the fluctuating terms of the model can only propagate upstream and eventually transform to triggered stop-and go waves while, near the downstream boundary, the congestion is essentially homogeneous and similar to the "synchronized traffic" state proposed by Kerner [39]. In contrast, the congested state of the IDMM simulation 4(a) is convectively unstable leading to oscillations also near the downstream boundary. Increasing T' from 1.2 s to 1.3 s in the simulation of Fig. 4(c) leads to convectively unstable traffic in this simulation as well and the macroscopic dynamics becomes even more similar to that of Fig. 4(a).

evtl. Bild $n_a = 5$, $T' = 1.3$ s?

2. *Virtual detector data*

Figure 5 shows flow-density data ("fundamental diagram") of a virtual detector at $x = 14$ km (5 km upstream of the bottleneck) with a sampling period of 1 min. In agreement with real traffic data [24], the data cover a two-dimensional area in the congested region, both for the IDMM [Fig. 5(a)] and for the HDM with finite reaction times and anticipations [Fig. 5(b)].

Since the HDM has a unique equilibrium flow-density curve and we simulated identical driver-vehicle combinations, the obseved scattering implies that the simulated congested traffic is out of equilibrium. In the simulations, possible forces bringing traffic out of equilibrium are (i)

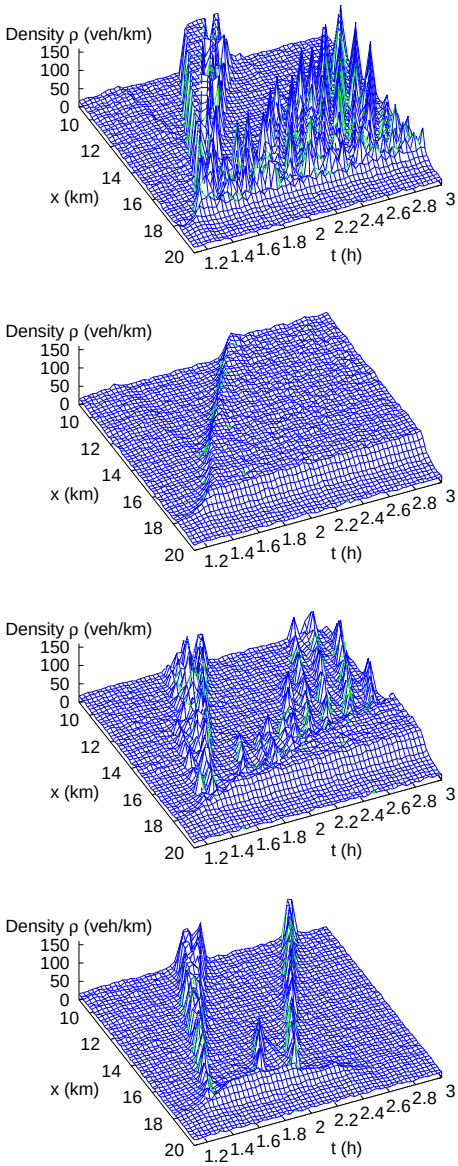

FIG. 4: Spatiotemporal dynamics of typical traffic states corresponding to the phase diagram Fig. 3. (a) $n_a = 1$, $T' = 0$ s (the special case of the IDMM) leading to OCT; (b) $n_a = 5$, $T' = 0.5$ s (HCT); (c) $n_a = 5$, $T' = 1.2$ s (TSG); (d) $n_a = 8$, $T' = 1.2$ s (MLC).

the fluctuating terms of the HDM, (ii) traffic instabilities. The distance from the equilibrium curve (and thus the area of the scattering) is increased by the long relaxation times back to equilibrium implied by the adaptation of the driver behaviour to the traffic environment (memory effect). It turns out that traffic instabilities contribute much more to the scattering of the flow-density data than the fluctuating terms. Notice, however, that in general

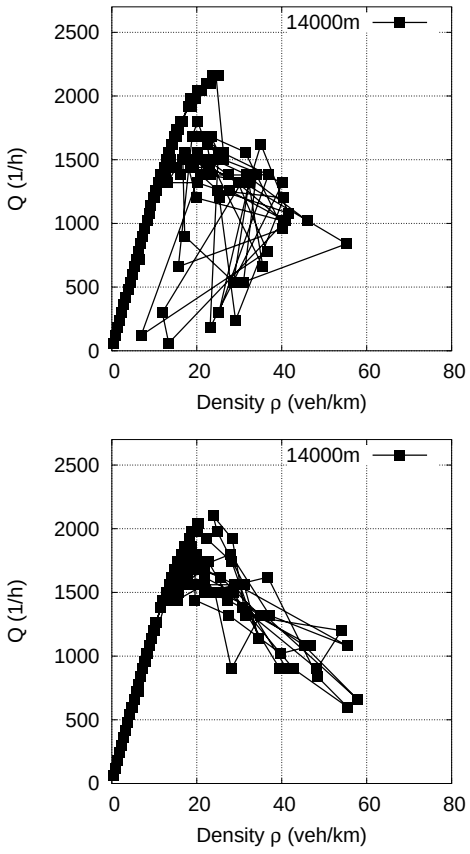

FIG. 5: Fundamental diagram as measured by a virtual detector (sampling interval $T_{\rm aggr} = 60$ s) at $x = 14.0$ km. (a) special case of the IDMM ($n_a = 1$, $T' = 0$ s) leading to OCT, (b) finite anticipations and reaction times ($n_a = 5$, $T' = 1.2$s) leading to TSG.

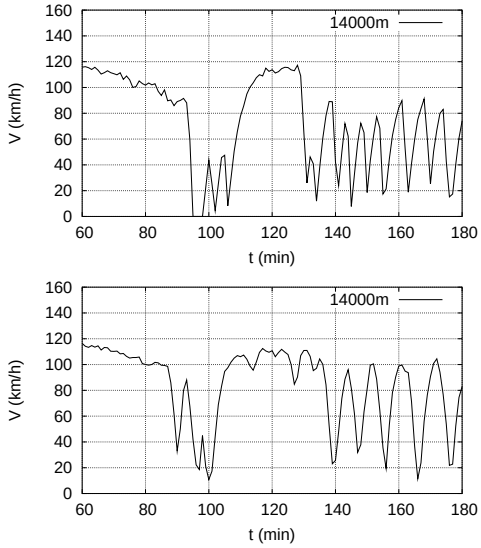

FIG. 6: Velocity time series from a virtual detector at $x = 14$ km for (a) $n_a = 1$, $T' = 0$ s, and (b) $n_a = 5$, $T' = 1.2$ s.

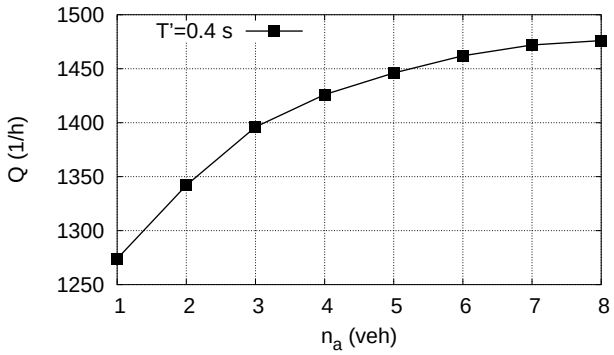

FIG. 7: Averaged outflow from the stationary downstream front of the congested area located at the bottleneck.

situations the heterogeneity of the driving styles and vehicle types plays an important role as well [18, 32, 40, 41] which is discussed in more detail in [17]. Figure 6 shows velocity time series of the same virtual detectors. Compared to the IDMM, the finite reaction times and anticipations of the HDM lead to a larger period of the velocity oscillations (about 10 min and 6 min for the HDM and IDMM, respectively) and to softer upstream fronts of congestions, i.e., to lower velocity gradients. Remarkably, the periods and gradients of the velocity time series of the HDM agree nearly quantitatively with that of real OCT data, cf, e.g., Fig. 12 in [26].

3. Dynamic capacity: Traffic outflow

We measured the averaged outflow $Q_{\rm out}$ from congested traffic at the downstream front located near the bottleneck using a virtual detector immediately downstream of the front at $x = 18750$ m. To average over the oscillations of OCT states. we used an increased sampling interval of $T_{\rm aggr} = 30$ min. Notice that $Q_{\rm out}$ can be considered as a dynamical road capacity [42].

Figure 7 shows $Q_{\rm out}$ as a function of the number of anticipated vehicles for a constant value $T' = 0.4$ s of the reaction time. Increasing the number of anticipated vehicles from $n_a = 1$ to $n_a = 5$ leads to an increase of the dynamical road capacity of about 15%. A further increase of *na* yielded no significant changes. Remarkably, up to $T' = 1.2$ s, the dynamic capacity $Q_{\rm out}$ depends only marginally on the reaction time. Increasing T' from 0.4 to 1.2 decreases $Q_{\rm out}$ by about 1% for all values of n_a where no crashes occur.

IV. DISCUSSION

Multi-anticipation to more than one front vehicle, anticipation of the future traffic situation, finite reaction

times, and errors in estimating distances and velocities are key aspects of the human driving behaviour.

In this work we proposed a general scheme to include these aspects into car-following models and applied it to the IDM resulting in the human-driver model (HDM). It is straightforward to use any other micromodel where the acceleration depends only on positions, velocities and accelerations of the own and the preceding vehicle such as the optimal-velocity model [11], the Gipps model [28], or the boundedly rational driver model [29, 30]. Since the underlying models have both the advantages and limitations of automatic cruise control (ACC) systems, one can investigate the impact of a wider distribution of ACC vehicles on the capacity and stability of the overall traffic simply by simulating a mixture of, e.g., IDM and HDM vehicles.

While finite reaction times has been investiagted as early as 1961 [10], the HDM is, to our knowledge, the first model allowing accident-free driving at realistic accelerations in all traffic situations for reaction times of the order of the time headway. The fact that this is a simple task for human drivers suggests that both spatial and temporal anticipations are important elements in human driving strategies.

Remarkably, it turned out that the destabilizing effects of finite reaction times and estimation errors can be offset to a large extent by the stabilizing effects of spatial and temporal anticipations. This explains why conventional car-following models such as the IDM can describe many features of observed traffic dynamics although they implement the driving style of machines, not humans. A closer look on quantitative features of stop-and-go traffic such as velocity gradients or the period of the oscillations, as recorded by virtual detectors, shows that the dynamics of the HDM agrees better with actual traffic data than that produced by car-following models. In the latter, the gradients typically are too large and the periods between two "stop" waves too short. Thus it seems that the large discrepancy between the "microscopic" time scales for adapting distances and velocities (of the order of 10 s) and the observed macroscopic time scales (of the order of 10 min or more for the period between two "stop" waves) are caused, at least partly, by multi-anticipations of the human drivers.

In addition to the congested states of the "phase diagram" of Helbing and Treiber [23], the HDM includes complex traffic breakdown scenarios such as the coexistence of free traffic, homogeneous congested traffic, and triggered stop-and go waves [Fig. 4(c)]. Such states, called "generalized patterns" in the nomenclature of Kerner [24] have been observed on some German freeways [24**?**]. **Bitte das Paper von Martin2 (empirische Verkehrszustaende) in die Datenbank eintragen, ggf. als Preprint** Simulations with the HDM suggest as general mechanism for such states an interplay between the fluctuations induced by the estimation errors and the macroscopic dynamics of congested traffic. If the congested traffic behind a bottleneck is convectively stable but linearly unstable [23], the small fluctuations grow while propagating opposite to the driving direction. Because the fluctuations cannot propagate in the driving direction, the congested traffic near the bottleneck is essentially homogeneous ("synchronized traffic") while further upstream the linear instability eventually triggers stop-and-go waves.

From a control-theoretic point of view, the HDM implements a continuous response to delayed and noisy input stimuli. Alternatively, human driving behaviour has been modelled by so-called action-point models where the response changes discontinuously whenever certain boundaries in the space spanned by the input stimuli are crossed [5, 43–45]. It has been proposed that distractions and the "restricted attention span" of human drivers play an important role in the driving behaviour as well [46]. In the HDM, a restricted attention can be modelled simply by increasing the update interval of the numerical Euler updates to values up to 1.5 s (cf. Fig. 2) and identifying the update interval as the typical time interval where the attention of the driver is not focussed on the traffic. Since the reaction time can be varied independently from the update interval, the combined effects of distractions and finite reaction times can be investigated simultaneously.

Finally it should be mentioned that, in this work, we considered only the longitudinal aspects (acceleration and deceleration) of human drivers and implemented only one vehicle-driver combination. Platooning effects due to different driving styles and the remarkable ability of human drivers to safely and smoothly change lanes even in congested conditions are the topic of a forthcoming paper.

Acknowledgments: The authors would like to thank for financial support by the DFG (grant No. He 2789).

[1] M. Brackstone and M. McDonald. Car-following: a historical review. *Transp. Res. F*, 2:181–196, 1999.

[2] D. Helbing. Traffic and related self-driven many-particle systems. *Review of Modern Physics*, 73:1067–1141, 2001.

[3] E.N. Holland. A generalised stability criterion for motorway traffic. *Transp. Res. B*, 32:141–154, 1998.

[4] H. Lenz, C.L. Wagner, and R. Sollacher. Multi-anticipative car-following model. *European Physical Journal*, B7:331–335, 1998.

[5] N. Eissfeldt and P. Wagner. Effects of anticipatory driving in a traffic flow model. *European Physical Journal B*, 33:121–129, 2003.

[6] C. Wagner. Asymptotic solutions for a multi-anticipative car-following model. *Physica A*, 260:218–224, 1998.

[7] L.C. Davis. Multi-lane simulations of traffic phases using a modified optimal-velocity model. *cond-mat??*, 2003.

[8] M. Treiber and D. Helbing. Microsimulations of freeway traffic including control measures. *Automatisierungstech-*

nik, 49:478–484, 2001.

[9] Johan Bengtsson. Adaptive cruise control and driver modeling. 2001.

[10] G.F. Newell. Nonlinear effects in the dynamics of car following. *Operations Research*, 9:209, 1961.

[11] M. Bando, K. Hasebe, A. Nakayama, A. Shibata, and Y. Sugiyama. Dynamical model of traffic congestion and numerical simulation. *Phys. Rev. E*, 51:1035–1042, 1995.

[12] M. Bando, K. Hasebe, K. Nakanishi, and A. Nakayama. Analysis of optimal velocity model with explicit delay. *Phys. Rev. E*, 58:5429, 1998.

[13] L.C. Davis. Comment on "analysis of optimal velocity model with explicit delay. *Phys. Rev. E*, 66:038101, 2002.

[14] L.C. Davis. Modifications of the optimal velocity traffic model to include delay due to driver reaction time. *Physica A*, 319:557, 2002.

[15] Benno Tilch and Dirk Helbing. Evaluation of single vehicle data in dependence of the vehicle-type, lane, and site. In D. Helbing, H.J. Herrmann, M. Schreckenberg, and D.E. Wolf, editors, *Traffic and Granular Flow '99*, pages 333–338. Springer, Berlin, 2000.

[16] W. Brilon and M. Ponzlet. Application of traffic flow models. In D. E. Wolf, M. Schreckenberg, and A. Bachem, editors, *Traffic and Granular Flow*, pages 23–40. World Scientific, Singapore, 1996.

[17] M. Treiber and D. Helbing. Memory effects in microscopic traffic models and wide scattering in flow-density data. *Phys. Rev. E*, 68:046119, 2003.

[18] Katsuhiro Nishinari, Martin Treiber, and Dirk Helbing. Interpreting the wide scattering of synchronized traffic data by time gap statistics. *Phys. Rev. E*, 68:067101, 2003.

[19] Dirk Helbing, Illés J. Farkas, Dominique Fasold, Martin Treiber, and Tamás Vicsek. Critical discussion of "synchronized flow" simulation of pedestrian evacuation, and optimization of production processes. In *Traffic and Granular Flow 2001*, page to appear. Springer, Berlin, 2002. TGF01?

[20] M. Treiber and D. Helbing, *Explanation of observed features of self-organization in traffic flow*, e-print cond-mat/9901239.

[21] P. G. Gipps. A behavioural car-following model for computer simulation. *Transportation Research B*, 15:105–111, 1981.

[22] Peter Hidas. Modelling lane changing and merging in microscopic traffic simulation. *Transportation Research C*, 10:351–371, 2002. MOBIL like model.

[23] D. Helbing, A. Hennecke, and M. Treiber. Phase diagram of traffic states in the presence of inhomogeneities. *Phys. Rev. Lett.*, 82:4360–4363, 1999.

[24] B.S. Kerner. Empirical macroscopic features of spatio-temporal traffic patterns at highway bottlenecks. *Phys. Rev. E*, 65:046138, 2002.

[25] D. Helbing and M. Treiber. Critical discussion of "synchronized flow". *Cooper@tive Tr@nsport@tion Dyn@mics*, 1:2.1–2.24, 2002. (Internet Journal, `www.TrafficForum.org/journal`).

[26] M. Treiber, Ansgar Hennecke, and D. Helbing. Congested traffic states in empirical observations and microscopic simulations. *Physical Review E*, 62:1805–1824, 2000.

[27] Elmar Brockfeld, R.D. Kühne, and Peter Wagner. Towards benchmarking microscopic traffic flow models. In W. Möhlenbrink, M. Bargende, U. Hangleiter, and U. Martin, editors, *FOVUS: Networks for Mobility 2002, International Symposium, September 18-20, 2002, Stuttgart*, pages 321–331. 2002.

[28] P. G. Gipps. *Transp. Res.*, 20 B:403, 1986.

[29] I. Lubashevsky, P. Wagner, and R. Mahnke. Bounded rational driver models. *EPJ B*, 32:243, 2003.

[30] Ihor Lubashevsky, Peter Wagner, and Reinhard Mahnke. Rational-driver approximation in car-following theory. *PRE*, 68:056109, 2003.

[31] L.C. Edie and R.S. Foote. Traffic flow in tunnels. In H.P. Orland, editor, *Highway Research Board Proceedings, 37th annual meeting*. National Academy of Sciences, Washington D.C., 1958.

[32] Martin Treiber, Ansgar Hennecke, and Dirk Helbing. Microscopic simulation of congested traffic. In D. Helbing, H.J. Herrmann, M. Schreckenberg, and D.E. Wolf, editors, *Traffic and Granular Flow '99*, pages 365–376. Springer, Berlin, 2000.

[33] Inclusion of the acceleration $a_{\alpha-1}(t)$ of the preceding vehicle to the input variables is straightforward allowing for micromodels that model reactions to braking lights.

[34] Generally, the estimation error concludes a systematic bias as well. We found that our model is very robust with respect to reasonable biases in distance and velocity-difference estimates.

[35] C.W. Gardiner. *Handbook of Stochastic Methods*. Springer, N.Y., 1990.

[36] Martin Treiber and Dirk Helbing. ??

[37] Minoru Fukui, Yuki Sugiyama, Michael Schreckenberg, and Dietrich E. Wolf (eds.). *Traffic and Granular Flow '01*. Springer, Berlin, 2003.

[38] D. Helbing, A. Hennecke, V. Shvetsov, and M. Treiber. Micro- and macrosimulation of freeway traffic. *Mathematical and Computer Modelling*, 35:517–547, 2002.

[39] B.S. Kerner and H. Rehborn. Experimental properties of phase transitions in traffic flow. *Phys. Rev. Lett.*, 79:4030–4033, 1997.

[40] J. H. Banks. An investigation of some characteristics of congested flow, 1998. J.H. Banks, An Investigation of some Characteristics of Congested Flow, Transportation Research Board, submitted 1998.

[41] M. Treiber and D. Helbing. Macroscopic simulation of widely scattered synchronized traffic states. *J. Phys. A*, 32(1):L17–L23, 1999.

[42] F.L. Hall and K. Agyemang-Duah. Freeway capacity drop and the definition of capacity. *Transportation Research Record*, 1320:91–108, 1991.

[43] P. Wagner and I. Lubashevsky. Empirical basis for car-following theory development. *cond-mat/0311192*, 2003.

[44] R. Wiedemann, *Simulation des Straßenverkehrsflusses*, Schriftenreihe des IfV Vol. **8**, Institut für Verkehrswesen, Universität Karlsruhe (1974).

[45] E. P. Todosiev. The action-point model of the driver-vehicle system. Technical report 202a-3, Ohio State University, Columbus, Ohio, 1963.

[46] E.R. Boer. Car followingfrom the driver's perspective. *Transp. Res. F*, 2:201–206, 1999.